Algorithm Theoretical Basis Document for Precipitating Clouds of the NWC/PPS

NWC/CDOP2/PPS/SMHI/SCI/ATBD/4, Issue 1, Rev. 0

15 September 2014

Applicable to SAFNWC/PPS version 2014

Applicable to the following PGE:s:

PGE	**Acronym**	**Product ID**	**Product name**	**Version number**
PGE04	PC	NWC-073	Precipitating Clouds	1.6

Prepared by Swedish Meteorological and Hydrological Institute (SMHI)

REPORT SIGNATURE TABLE

Function	Name	Signature	Date
Prepared by	SMHI		15 September2014
Reviewed by	SAFNWC Project Team EUMETSAT		9 September 2014
Authorised by	Anke Thoss, SMHI *SAFNWC PPS Manager*		15 September 2014

DOCUMENT CHANGE RECORD

Version	Date	Pages	Changes
1.0d	22 January 2014	35	Replacing CDOP-document: SAF/NWC/CDOP/SMHI-PPS/SCI/ATBD/4 First version for SAFNWC/PPS v2014 Changes since v2012: Updated the output description, and some minor general improvements.
1.0	15 September 2014	36	Implemented RIDs from PCR-v2014: -LSc1 (formal issues) -LSc2 (summary of requirements) -LSc3, LSc5 (editorials)

Table of Contents

List of Tables and Figures

1. INTRODUCTION

The EUMETSAT "Satellite Application Facilities" (SAF) are dedicated centres of excellence for processing satellite data, and form an integral part of the distributed EUMETSAT Application Ground Segment (http://www.eumetsat.int). This documentation is provided by the SAF on Support to Nowcasting and Very Short Range Forecasting, SAFNWC. The main objective of SAFNWC is to provide, further develop and maintain software packages to be used for Nowcasting applications of operational meteorological satellite data by National Meteorological Services. More information can be found at the SAFNWC webpage, http://www.nwcsaf.org . This document is applicable to the SAFNWC processing package for polar orbiting meteorological satellites, SAFNWC/PPS, developed and maintained by SMHI (http://nwcsaf.smhi.se).

1.1 PURPOSE

This document is the Algorithm theoretical Basis Document for the PGE04 (PC, Precipitating Cloud) of the SAFNWC/PPS software package.

This document contains a description of the algorithm, including scientific aspects and practical considerations.

1.2 SCOPE

This document describes the algorithms implemented in the PGE04 version v1.6 of the 2014 SAFNWC/PPS software package delivery.

1.3 DEFINITIONS AND ACRONYMS

Acronym	Explanation
ACPG	AVHRR/AMSU Cloud Product Generation software (A major part of the SAFNWC/PPS s.w., including the PGE:s.)
AEMET	Agencia Estatal de Meteorología (Spain)
AHAMAP	AMSU-HIRS-AVHRR Mapping Library (A part of the SAFNWC/PPS s.w.)
AMSU	Advance Microwave Sounding Unit
AVHRR	Advanced Very High Resolution Radiometer
CDOP	Continuous Development and Operational Phase
CDOP-2	Second Continuous Development and Operational Phase
CMA	Cloud Mask (also PGE01)
CPP	Cloud Physical Products
CT	Cloud Type (also PGE02)
CTTH	Cloud Top Temperature, Height and Pressure (also PGE03)
EPS	EUMETSAT Polar System
EUMETSAT	European Organisation for the Exploitation of Meteorological Satellites
FAR	False Alarm Rate
FOV	Field Of View
GEO	Geosynchronous equatorial orbit
IR	Infrared
LEO	Low Earth orbit
LUT	Look-up-table
MHS	Microwave Humidity Sounding Unit
NIR	Near Infrared
NOAA	National Oceanic and Atmospheric Administration
NORDRAD	Nordic Weather Radar Network
NWP	Numerical Weather Prediction
PC	Precipitating Cloud (also PGE04)
PCPN	Precipitation
PGE	Process Generating Element
PI	Precipitation Index
POD	Probability Of Detection
PODF	Probability Of False Detection
PPS	Polar Platform System
RGB	Red Green Blue
SAF	Satellite Application Facility
SAFNWC	Satellite Application Facility for support to NoWcasting
SI	Scattering Index
SMHI	Swedish Meteorological and Hydrological Institute
TBC	To Be Confirmed
TBD	To Be Defined
TOA	Top Of Atmosphere
USGS	U.S. Geological Survey
VIIRS	Visible Infrared Imaging Radiometer Suite
VIS	Visible

See [RD.1] for a complete list of acronyms for the SAFNWC project.

1.4 REFERENCES

1.4.1 Applicable documents

The following documents, of the exact issue shown, form part of this document to the extent specified herein. Applicable documents are those referenced in the Contract or approved by the Approval Authority. They are referenced in this document in the form [AD.X]

For dated references, subsequent amendments to, or revisions of, any of these publications do not apply. For undated references, the current edition of the document referred applies.

Current documentation can be found at SAFNWC Helpdesk web: http://www.nwcsaf.org

Ref	Title	Code	Vers	Date
[AD.1.]	NWCSAF Project Plan	NWC/CDOP2/SAF/AEMET/MGT/PP	1.2	28/06/13
[AD.2.]	NWCSAF Product Requirements Document	NWC/CDOP2/SAF/AEMET/MGT/PRD	1.5	05/06/14
[AD.3.]	System and Components Requirements Document for the SAFNWC/PPS	NWC/CDOP2/PPS/SMHI/SW/SCRD	1.0	15/09/14

Table 1: List of Applicable Documents

1.4.2 Reference documents

The reference documents contain useful information related to the subject of the project. These reference documents complement the applicable ones, and can be looked up to enhance the information included in this document if it is desired. They are referenced in this document in the form [RD.X]

For dated references, subsequent amendments to, or revisions of, any of these publications do not apply. For undated references, the current edition of the document referred applies

Current documentation can be found at SAFNWC Helpdesk web: http://www.nwcsaf.org

Ref	Title	Code	Vers	Date
[RD.1]	The Nowcasting SAF Glossary	NWC/CDOP2/SAF/AEMET/MGT/GLO	2.0	18/02/14
[RD.2]	Validation Report for v.2008 of the SAFNWC/PPS	SAF/NWC/CDOP/SMHI-PPS/SCI/VR/1	2.1.1	19/03/08
[RD.3]	Output Data Format of the SAFNWC/PPS	NWC/CDOP2/PPS/SMHI/SW/DOF	1.1	15/09/14
[RD.4]	Algorithm Theoretical Basis Document for Cloud Type of the NWC/PPS	NWC/CDOP2/PPS/SMHI/SCI/ATBD/2	1.0	15/09/14
[RD.5]	User Manual for the NWC/PPS application: Software Part, 2.Operation	NWC/CDOP2/PPS/SMHI/SW/UM/2	1.0	15/09/14

Table 2: List of Referenced Documents

1.4.3 Scientific references

Antonelli, P., 2007: Final Report on the Visiting Silent Activity: Refinement and Operational Implementation of a Rain Rate Algorithm based on AMSU-A/MHS and rain gauge data over the H-SAF Area. *EUMETSAT Visiting Scientist Report***,** 55 pages.

Bennartz, R., 2007: Extending the NWCSAF PC Product to include precipitation rate. SAFNWC Visiting Associate Scientist Final Report, July 2007.

Bennartz, R., 2000: Optimal convolution of AMSU-B to AMSU-A. *Journal of Atmospheric and Oceanic Technology*, **17,** 1215-1225.

Bennartz, R. and G. W. Petty, 2001: The sensitivity of microwave remote sensing observations of precipitation to ice particle size distributions. *Journal of Applied Meteorology*, **40,** 345-364.

Bennartz, R. and D. B. Michelson, 2003: Correlation of precipitation estimates from spaceborne passive microwave sensors and weather radar imagery for BALTEX PIDCAP. *International Journal of Remote Sensing*, **24,** 723-739.

Bennartz, R., A. Thoss, A. Dybbroe, and D. B. Michelson, 2002: Precipitation analysis using the Advanced Microwave Sounding Unit in support of nowcasting applications. *Meteorological Applications*, **9,** 177-189.

Bennartz R., SAFNWC Precipitating Clouds product extension to new generation MW sensors and products validation. SAFNWC Visiting Associate Scientist Final Report, July 2006.

Bennartz, R., Thoss, A., Dybbroe, A., and Michelson, D., 1999. Precipitation Analysis from AMSU. Reports Meteorologi 93, SMHI, Folborgsvägen 1, SE-60176 Norrköping, Sweden. NWCSAF Visiting Scientist Report.

Rinehart, R. E., RADAR for Meteorologists, Third Edition, ISBN 0-9658002-0-2, Rinehart Publications 1997.

Thoss, A., 2002. Delta development for the MSG PGE04, Feasability of including the 1.6µm channel. Technical report, SMHI.

Thoss, A. and Dybbroe, A., 2001. The Nowcasting SAF Precipitating Clouds Product. In *Proceedings of the 2001 EUMETSAT Meteorological Satellite Data Users' Conference, Antalya, Turkey 1-5 Oct.*, pp. 399.406.

1.5 Document Overview

This document contains a theoretical description of the algorithms for Precipitating Clouds derivations. The document has been structured in the following sections:

- Section 1 contains the current introduction along with the list of used acronyms and applicable and reference documents.
- Section 2 A short overview of the precipitating clouds algorithm
- Section 3 Algorithm description in more detail
- Section 4 A description of known problems and limitations
- Section 5 Practical aspects, like input, output and configuration.

1.6 Scientific Updates since PPS Version 2012

For v2014 PGE04 has not undergone a certain scientific update in terms of changing the algorithm. However, it is noteworthy that the output has been harmonized in general with the respectively output from GEO algorithms.

2. ALGORITHM OVERVIEW

The Precipitating Clouds product is aimed for Nowcasting applications. It shall give the forecaster a quick overview over the probability of precipitation in a few coarse intensity intervals. Important features are that the scheme shall work seamlessly over land and sea and shall work for day and night and for both stratiform and convective cases. The product can be used by the forecaster as a complement to radar data, especially in areas without radar coverage.

The information content of AVHRR data (or corresponding VIIRS channels) with respect to precipitation is somewhat limited, especially for stratiform cases, where it is often difficult to distinguish between precipitating and non-precipitating parts of a cloud system. The algorithm is therefore complemented by information from the AMSU and MHS instrument on board the NOAA and Metop satellites.

The scattering signature at microwave frequencies of 89GHz and 150GHz/157GHz is caused by frozen precipitation sized particles and is thus physically more directly coupled to precipitation generating processes than signatures in VIS or IR channels. Neither AVHRR nor AMSU are specifically designed for precipitation retrieval and precipitation estimates from these instruments inhibit some uncertainty. Rather than trying to estimate rain rates with big associated errors it was felt more adequate for Nowcasting applications to estimate the precipitation likelihood in three intensity intervals for light, medium and heavy precipitation.

Both the AVHRR and the AMSU part of the algorithm are statistically derived by comparing features sensitive to precipitation with radar estimated rain rates. In the AVHRR part of the algorithm a Precipitation Index PI is constructed as a linear combination of spectral features correlated with precipitation. For each possible value of the PI the probability of precipitation has been estimated from a comprehensive set of radar/satellite collocations. In the MW part of the algorithm a Scattering Index SI is constructed from the differences of the 89GHz and 150GHz/157GHz channels and related to precipitation in an equivalent manner as for the PI. The two likelihood estimates are then combined in a sequence of decisions determining for each AVHRR pixel whether the AVHRR or MW estimate is selected. AVHRR is mainly used for quality control of AMSU by screening out spurious light precipitation from AMSU and to supplement the estimates where no MW data is available (as in between AMSU footprints and at the sides of the satellite swath). The product can also be configured not to use any MW data. For more possibilities of configuration consult section 5.2 on configuration.

The nature of the input data allows only a rough classification of precipitation likelihood into four precipitation classes:

- Class 0: No precipitation 0.0 - 0.1 mm/h
- Class 1: Very light precipitation > 0.1 - 0.5 mm/h
- Class 2: Light to moderate Precipitation > 0.5 - 5.0 mm/h
- Class 3: Heavy precipitation > 5.0 mm/h

The likelihood in all four classes has to sum up to 100%. The total likelihood of precipitation is the sum of the likelihood in classes one to three. Since all information is already contained in classes one to three, no output is given for class0, which thus can be calculated by 100% - total precipitation likelihood.

2.1 REQUIREMENTS

The requirements for the SAFNWC/PPS products are described in the Product Requirements Document [AD.2.]. In Table 3 is given a summary of the requirement specific for the precipitating clouds product.

Table 3 Accuracy requirements for Precipitating Clouds

	POD	**FAR**
Threshold accuracy	55%	70%
Target accuracy	65%	65%
Optimal accuracy	80%	50%

3. ALGORITHM DESCRIPTION

3.1 PROCESSING STEPS

3.1.1 Pre-processing of MW data

The first step in the PC algorithm is a pre-processing of the AMSU data. If AMSU use is requested, the precipitation likelihood from AMSU is retrieved for the whole swath and written to a file, which later serves as input to the main PC module. This calculation is done when the first region is processed and AMSU data use is enabled. In this pre-processing step, a scattering index (SI) is calculated from the difference between a high frequency AMSU channel and a lower frequency AMSU channel which is less affected by scattering from big ice particles. Different algorithms to derive an SI are implemented, depending on the surface type (land/sea) in the AMSU FOV. Using a comprehensive set of co-located radar derived rain rates, the SI is then related to precipitation probability in different intensity intervals. This pre-processing is done once for the satellite swath and the resulting file is subsequently read in by the main module. The pre-processing is described in more detail in section 3.1.1. Calculation of the background brightness temperatures is (from PGE04 v1.3 onward) done only from the individual overpasses and is allowed to vary more within the overpass area. This is accomplished via a sequence of operation performed on the two-dimensional fields of 89 GHz and 150 GHz brightness temperatures for each overpass. The background brightness temperatures are not calculated globally on the overpass. It is done for each scan line and the background brightness temperatures are calculated separately, so that latitudinal changes in surface characteristics are explicitly accounted for. This is done separately for land and water. Afterwards, each pixel is assigned a background brightness temperature weighted according to its fraction of land surface. The algorithm flow is outlined in Figure 1**.**

From NOAA-18 onward and for Metop satellites, the AMSU-B instrument was replaced by MHS with slightly different channel characteristics. The algorithm was adapted to this new instrument by applying a correction to the changed channel (157GHz for MHS instead of 150GHz for AMSU-B). Changes are described in Bennartz(2006), available on the NWCSAF websites and summarized in SAF/NWC/IOP/SMHI-PPS/SCI/RP/3. In this document, AMSU-B refers to both AMSU-B and MHS if not explicitly named otherwise and 150GHz refers to adjusted 157GHz brightness temperatures when applicable to the MHS sensor.

3.1.2 Main module

In the main module the output file from the pre processing is read in and the MW precipitation estimates are projected on AVHRR resolution. The precipitation likelihood is estimated from the AVHRR and finally merged with the MW estimate.

Pixels are processed in sequential order, following the rough steps:

- Is the Cloud Type class assigned to the pixel regarded as potentially precipitating? (see section 3.3.1) If yes: proceed, otherwise total precipitation likelihood for the pixel assigned to 0%.
- Calculate the precipitation index PI from AVHRR data and assign corresponding precipitation likelihood (see section 3.3.2). If the total precipitation likelihood from AVHRR

exceeds a threshold (recommended 10%, representing 5%-<15%), check whether valid MW precipitation estimate is available for that pixel

- If MW estimate is available, replace the AVHRR estimate with the MW estimate

The algorithm outlined above combines the respective advantages of both AVHRR and AMSU. The main advantage of AVHRR data for precipitation detection is its high spatial resolution. This enables for example the detection of even small convective cells. Another advantage is that cloud free areas as well as areas with cloud types which have an overall low likelihood to precipitate can easily be identified. However, since there is no strong coupling between spectral features and precipitation, the area of potential precipitation is overestimated, which leads in turn to fairly low precipitation probabilities. A stronger coupling exists between the scattering signatures detected by AMSU and precipitation. Rain areas can be better delineated than with AVHRR and overall likelihood for precipitation and intensity information is more decoupled, which allows to clearly identifying precipitation maxima. Usually the precipitation in frontal systems is better identified by AMSU, correctly reducing the area with potential precipitation with respect to the AVHRR estimate. However, sometimes spurious light precipitation may be detected by the AMSU algorithm, even in cloud free areas. Many of these areas are correctly screened out in the combined AVHRR/AMSU algorithm since no AMSU estimate is requested if the AVHRR classifies an area as precipitation free.

3.2 Microwave Algorithm

The AMSU consists of two instruments, AMSU-A and AMSU-B. While the former is dedicated to derive temperature profile information, it is no longer employed in the deriving the PC product. AMSU-B was designed for the retrieval of water vapour profile information. AMSU-B instrument is cross-track scanning and its swath consists of 90 measurements (step angle 1.1 degrees). AMSU-B has a spatial resolution of approx. 16 km at nadir. Details on the spatial resolution and observation geometry of the AMSU can be found in Bennartz (2000). From NOAA-18 onward and for Metop, the AMSU-B instrument has been replaced by the MHS instrument. AMSU-B has window channels at 89.0 and 150.0 GHz. MHS contains a high frequency window channel at 157GHz with very similar characteristics to the 150GHz channel. A correction for the MHS 157 GHz channel to emulate the AMSU-B 150GHz channel has been developed by Bennartz (2006) and proved to work fully satisfactory. The correction Makes additional use of the 183+7 GHz MHS channel:

$$Corr = a_0 + a_1 * T_{89} + a_2 * T_{183+7} + a_4 * \frac{T_{89}}{\cos(\theta)} \qquad \textit{Eq 1}$$

where θ is the observation zenith angle. The coefficients a are given in the Table 4 below. The correction term is then simply added to the 157 GHz brightness temperature.

Coefficient	Value
a_0	-0.4060
a_1	-0.1152
a_2	+0.1046
a_3	+0.00161

Table 4: Coefficients to correct MHS channel 2 within the SAFNWC-PC product.

The 89GHz and 150GHz (157GHz) channels are most suitable to obtain information about precipitation since they are least affected by water vapour or oxygen absorption. The response of passive microwave sensors to precipitation is qualitatively well known (Smith et al., 1998), while an exact quantitative relation between surface rain rate and observed brightness temperatures is difficult to establish. Considering the microwave response to precipitation two different signals have to be distinguished. First, liquid precipitation acts as an almost unpolarised emitter, so that the liquid precipitation over cold, polarised targets (i.e., water surfaces) tends to brighten and depolarise the satellite-observed temperatures. This effect can be observed especially at low frequencies, and its use is limited to open water surfaces, since most land surfaces exhibit surface emissivities which are too high and variable.

The second effect is a depression of the observed brightness temperatures which is largely caused by precipitation-sized ice particles (Spencer et al., 1989, Grody 1991, Adler et al., 1993). At high frequencies these large ice particles scatter cold radiation from above the cloud back to the satellite. While only indirectly linked with surface precipitation, the scattering signal can be observed both over land and water surfaces. For the special case of the AMSU the usage of the higher AMSU-B frequencies is advantageous because of its approximately three times higher spatial resolution. AMSU-B will therefore have a more dynamic response to precipitation features, especially, if the area extent of the precipitation is small.

The approach employed here to retrieve precipitation from AMSU makes use of the scattering signature at high frequencies. This enables us to retrieve precipitation over both water and land and also takes advantage of the higher spatial resolution of AMSU-B. The scattering index makes use of a predicted brightness temperature (T*) in the absence of scattering, which is derived from low frequency channels. The functional relationship between the low frequency brightness temperature (T_{low}) and T* can either be found by inverse radiative transfer modelling, or by global brightness temperature statistics. From T* the high frequency brightness temperature (T_{high}) is subtracted:

$$SI = T^*(T_{low}) - T_{high} \qquad \textit{Eq 2}$$

with SI being the scattering index, T_{low}, T_{high} being the observed low and high frequency brightness temperatures. Previous versions of the software were using different channel combinations over land, sea and coastal areas, explicitly, AMSU-A's 89 GHz and 23 GHz channels and AMSU-B's 89 GHz and 150 GHz (157GHz) channels. The latest version of this software (version 1.3) has a more simplified approach using the difference of AMSU-B/MHS higher frequency water vapour channels. The older parts of the code were, however, retained since we want to keep the option of activating it again, especially in light of the fact that the 89 GHz MHS channel on NPP/JPSS satellites will no longer exist.

Calculation of the background brightness temperatures is (from PGE04 v1.3 onward) done only from the individual overpasses and is allowed to vary more within the overpass area. This is accomplished via a sequence of operation performed on the two-dimensional fields of 89 GHz and 150 GHz brightness temperatures for each overpass. The background brightness temperatures are not calculated globally on the overpass. It is done for each scan line and the background brightness temperatures are calculated separately, so that latitudinal changes in surface characteristics are explicitly accounted for. This is done separately for land and water. Afterwards, each pixel is assigned a background brightness temperature weighted according to its fraction of land surface. The algorithm flow is outlined in Figure 1.

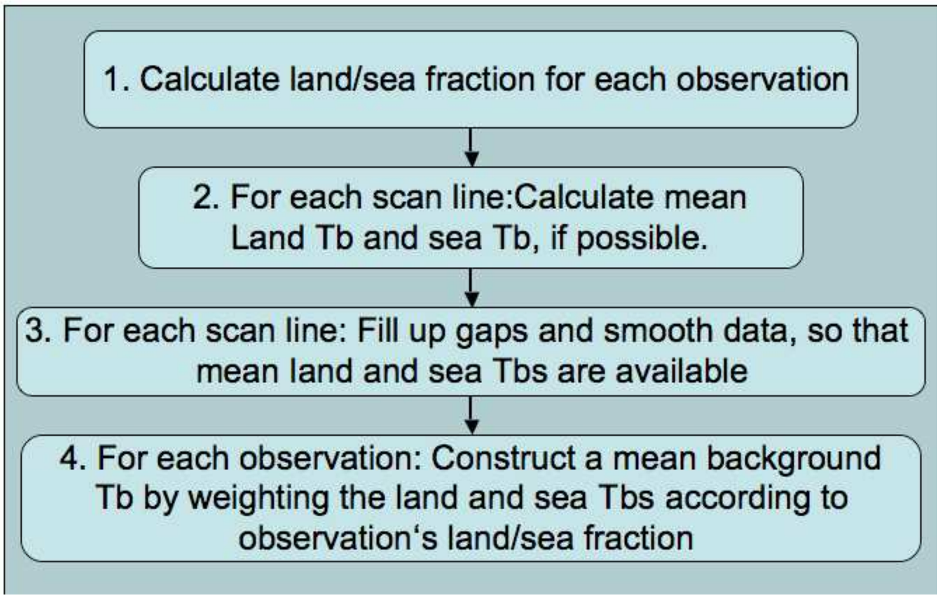

Figure 1: General algorithm flow of the calculation of background brightness temperatures.

This algorithm has, however, the disadvantage that longitudinal changes of surface emissivity for land or water surfaces are not accounted for. If, for example, to the left side of the scan sea ice is present, and to the right side open water, the algorithm will assign a mixture of both to determine the background. This will lead to misclassifications. The same holds for changes in land surface emissivity for example due to snow cover or different vegetation types. Note, that changes in land surface temperature are *not* as important as changes in surface emissivity, since the precipitation classification algorithm uses temperature differences between 89 GHz and 150 GHz and not absolute temperatures.

3.2.1 Statistically Derived Look-Up Tables

In order to associate the SI to precipitation intensity classes, collocated radar data was used. NORDRAD radar composites with instantaneous profile-corrected and quality controlled radar reflectivies are available starting 05/2006. These fields employ a new and more consistent gauge adjustment technique and in general provide a homogeneous precipitation estimate. The NORDRAD coverage area is shown in Figure 2.

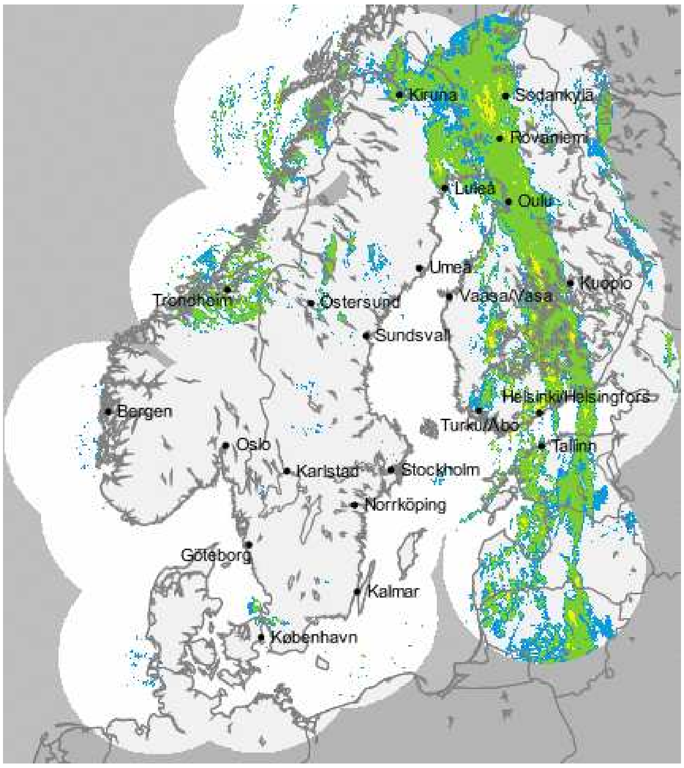

Figure 2: Sample radar image showing the NORDRAD coverage area.

Figure 3 gives an overview on the general observation geometry. Parallax errors as well as the approximately Gaussian shape of the passive microwave antenna pattern function (Bennartz, 2000) are taken into account.

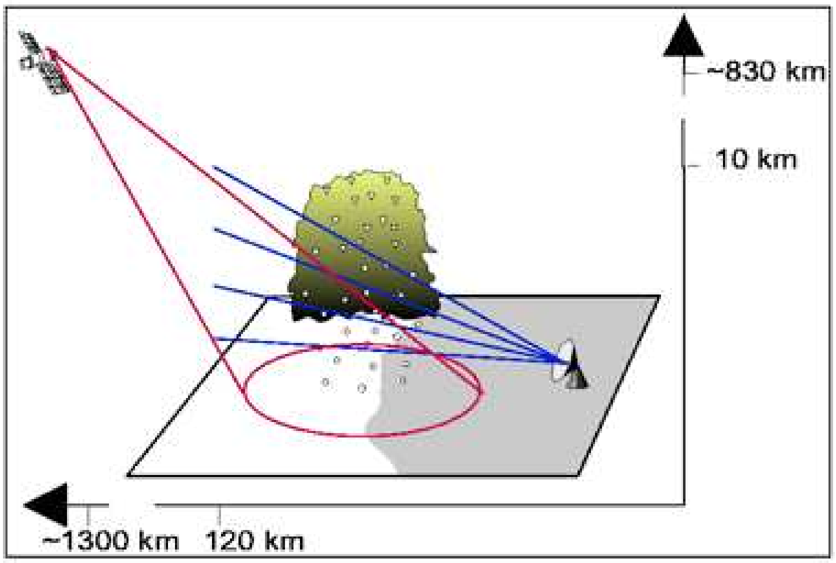

Figure 3: General observation geometry for convolution of NORDRAD data and land-sea masks to AMSU footprint size. Figure from (Bennartz and Michelson, 2003).

The relationship between linear radar reflectivity and rain rate is given by the Eq 3 and Eq 4 below.

$$Z = 10 \times \log_{10}\left(\frac{z}{1\,mm^6/m^3}\right) \qquad \textit{Eq 3}$$

$$z = 200 \times R^{1.5} \qquad \textit{Eq 4}$$

This Z-R (eq 3) relation is used at SMHI and therefore was the first choice of this study. It was necessary to convert the radar logarithmic reflectivity (dBZ) values to linear values before the rain rate relationship could be applied[1] .

The collocation radar data set stratified after land/sea and satellite is characterized in Table 5.

	Period	# Overpasses	# Obs. Land	# Obs. Sea
NOAA-15	1.6.06-31.5.07	1441	1.095.546	1.097.853
NOAA-17	23.6.07-31.12.07	1284	965.095	964.920
NOAA-18	1.6.06-31.5.07	1589	1.140.755	1.140.973

[1] The conversion formula was taken from RADAR for Meteorologists, Ronald E. Rinehart, Ph.D.

Metop-02	1.3.07-6.6.07	239	179.751	178.314

Table 5: Observation period and number of collocated satellite/radar observations for the four sensors under investigation. Individual observations were flagged as land, if the fraction of land within the 85 GHz footprint was greater as 95 %. Observations were flagged as 'sea', if the fraction of land within a 85 GHz footprint was smaller than 2 %.

The following figures show the results of this classification for land and water. From this data, two look-up tables are created to be used to associate each SI with the respective precipitation likelihood for all intensity classes.

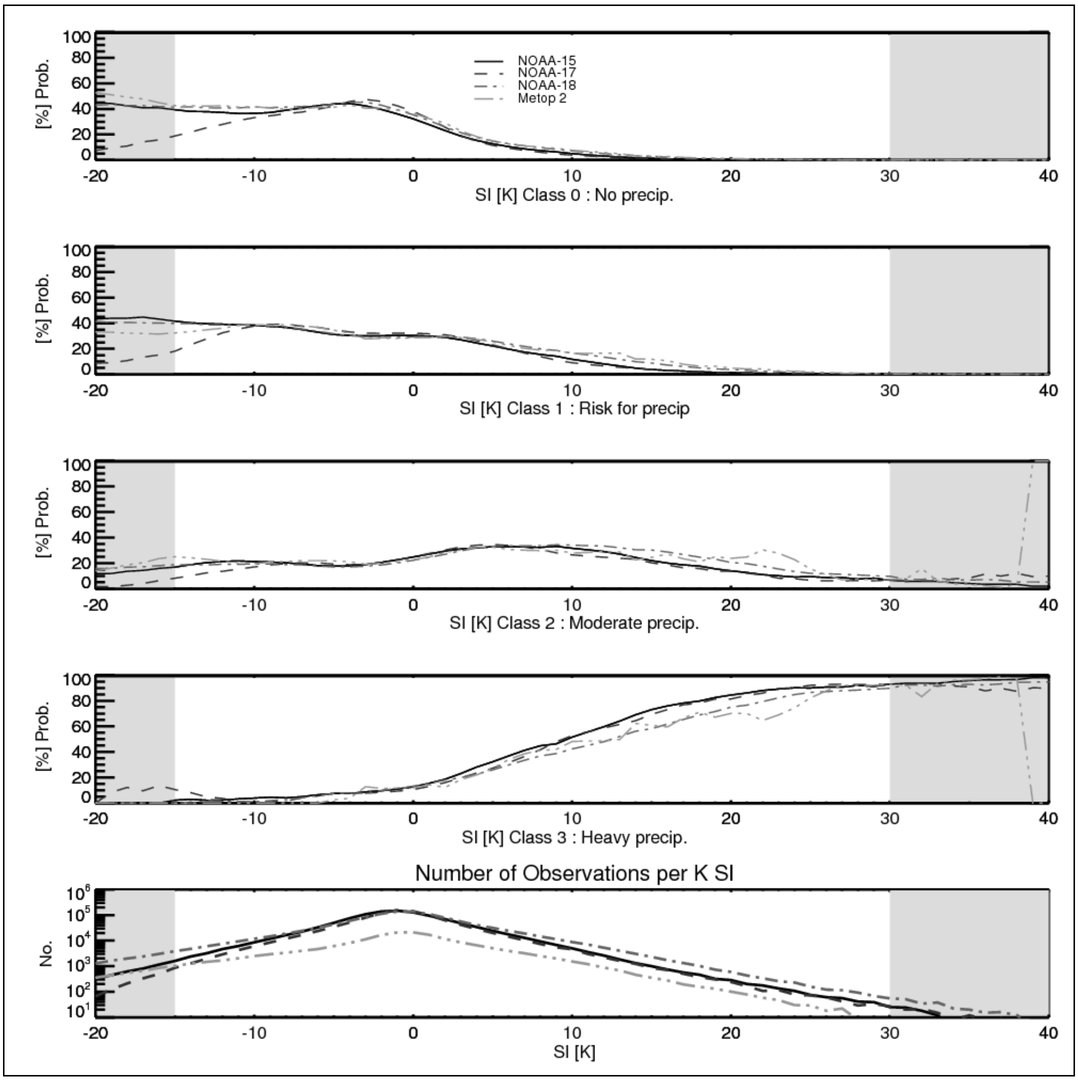

Figure 4: The four upper panels show the likelihoods of occurrence for the four different precipitation classes defined in the PC product over land. The lower plot gives the frequency of occurrence of observations at a given scattering index. The grey shaded areas show regions with low data density.

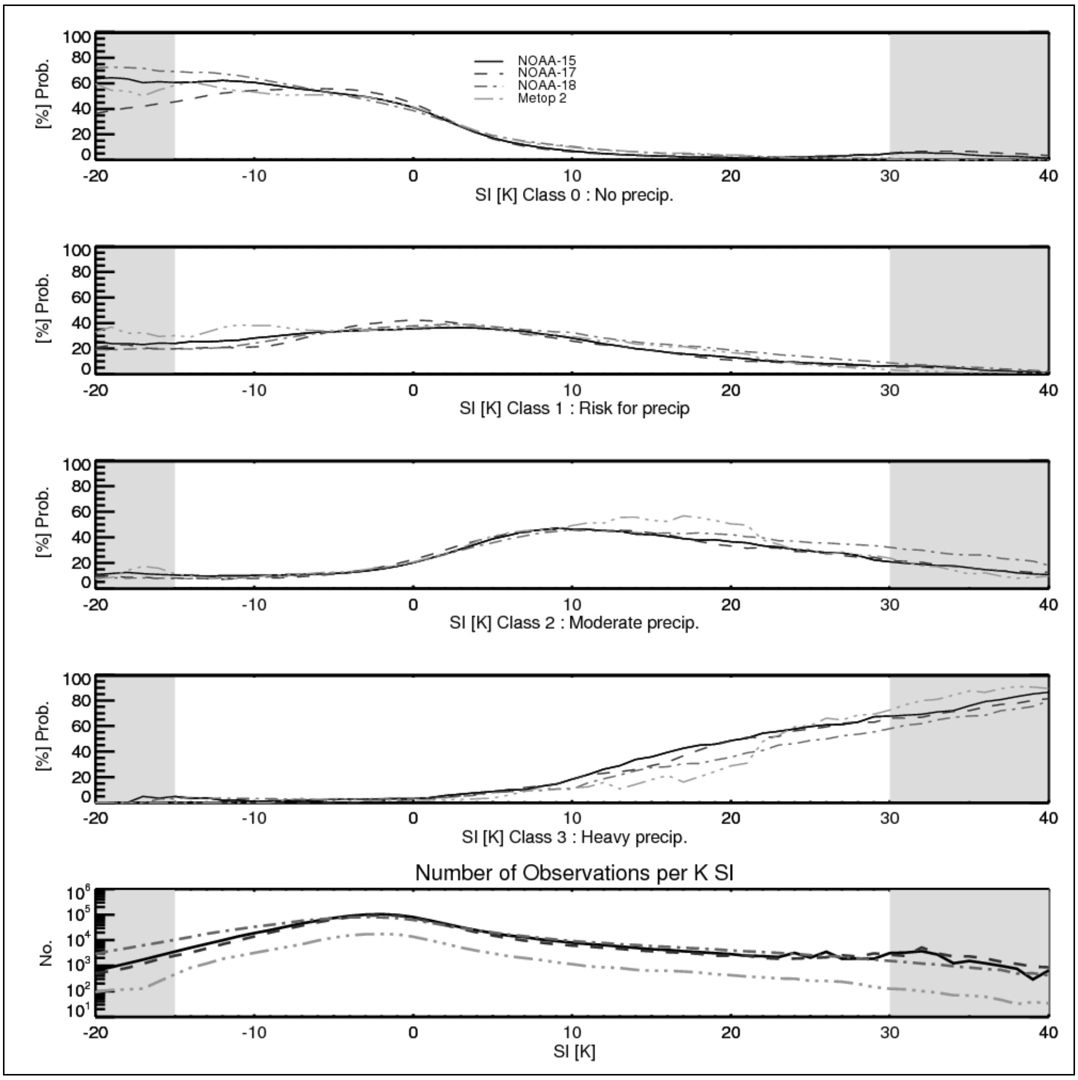

Figure 5: The same as Figure 4, except that this is over water.

In Figures: Figure 4 and Figure 5 it is easy to see how the SI varies for each class depending on the underlying surface type. The sum of all four classes must always equal 100%. It can be seen that adjacent precipitation classes overlap substantially. From left to right, the SI increases from -40 to 60 K. High negative values have statistically corresponded to dry condition with a change beginning around -20 K (when light precipitation steps into the picture) and peaks, for water cases, around 0K, while over land, the peak is around -5 K. This makes it quite likely that misclassification will occur between these classes when the SI lies between -5 and 20 K. Over land, the light precipitation class is a bigger problem: there is no strong peak, but rather a plateau from ~-20 to ~5 K. This means that more light precipitation cases will be misclassified over land than over the water. Unfortunately, the peak for the moderate precipitation lies relatively close by as well. The proximity of the moderate peak means that a SI between -5 and 15K risk being misclassified as light and visa versa. For the heavy precipitation class, it is should not be that easily affected as the likelihood increases with large positive SI values while the remaining categories taper off.

3.3 IR/VIS ALGORITHM

3.3.1 Screening according to cloud type

Cloud free areas and areas with cloud types that are rarely associated with precipitation according to radar are a-priori excluded from the precipitation estimation and assigned a total precipitation likelihood of 0%. Also different cloud types differ in the spectral features that are most correlated with precipitation. In the equation for calculating the PI we use coefficients which can vary according to cloud type to account for this effect. Which cloud classes are assumed to be potentially precipitating can be configured, as well as which specific algorithm (algorithm means here a set of coefficients and a corresponding specific table associating PI to precipitation likelihood) to use for calculating the PI and mapping it to precipitation likelihood. Figure 6 gives the statistic over rain frequency of cloud classed for 2007. Note that precipitation values for precipitating cloud classes are generally lower than that, described in Table 6 , since no gauge adjustment of radar rain rates was applied for Figure 6.

Ct No.	Description	pot. raining	Algorithm No.	rain acc. to radar
1	Cloud free land	No	0	2.6%
2	Cloud free sea	No	0	1.8%
3	Snow contaminated land	No	0	1.6%
4	Snow contaminated sea	No	0	1.0%
5	Very low cloud cumuliform	No	0	n.a.
6	Very low cloud stratiform	No	0	2.1%
7	Low cloud cumuliform	No	0	n.a.
8	Low cloud stratiform	No	0	5.6%
9	Medium level cloud cumuliform	Yes	1	n.a.
10	Medium level cloud stratiform	Yes	0	21.2%
11	High opaque cloud cumuliform	Yes	2	n.a.
12	High opaque cloud stratiform	Yes	2	38.9%
13	Very high opaque cumuliform	Yes	2	n.a.
14	Very high opaque stratiform	Yes	2	47.0%
15	Very thin cirrus	No	0	4.9%
16	Thin cirrus	Yes	3	8.4%
17	Thick cirrus	Yes	3	11.1%
18	Cirrus over lower clouds	Yes	4	16.6%
19	Fractional clouds	No	0	3.5%

Table 6: Precipitation statistics for PPS cloud types according collocated instantaneous radar in the Baltic area. 120 scenes were selected spanning one year. The radar data has been gauge adjusted. It is indicated whether a cloud type is treated as potentially raining (threshold currently set at 5% total precipitation likelihood) and which cloud type specific algorithm number is applied.

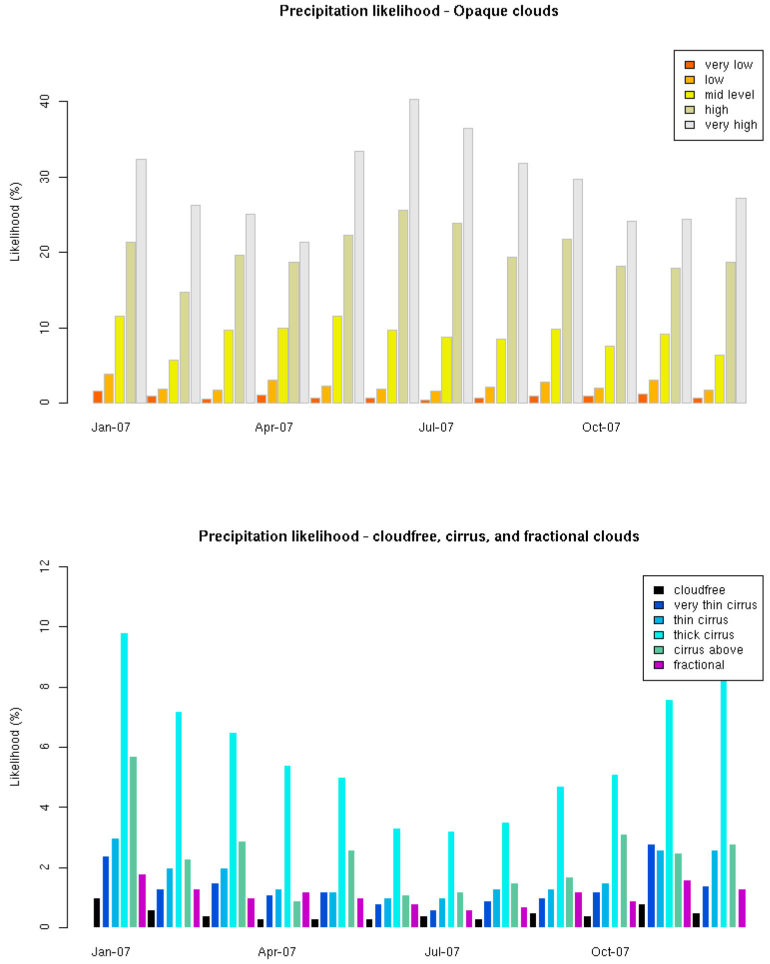

Figure 6: Percent likelihood for precipitation for each Cloud Type category, during the period January 2007 to December 2007. Precipitation is defined by an instantaneous radar reflectivity higher than 10 dBz. The 4 cloudfree classes have been gathered in one group and is represented by a black bar. No gauge adjustment is applied to the radar data

3.3.2 Precipitation Index and likelihood assignment

During daytime either the 1.6µm channel (3A) or 3.7µm channel (3B) is activated on board the NOAA satellites. Since the signal in both channels is strongly influenced by the microphysical state at the cloud top, we try to take advantage of these channels when possible. We found however, that the use of one visible channel (we chose 0.6µm) in the day time algorithms was sufficient, since the 0.8µm channel did not add additional information. Thus we needed to develop three classes of algorithms:

- Day time algorithm using 1.6µm (day 3A)
- Day time algorithm using 3.7µm (day 3B)

- Night time algorithm (night)

For each day or night class we also consider a cloud type dependence. Probability of rain is assigned according to cloud class and is derived by collocating satellite data with radar data. The cloud classes are categorized by their potential rain intensity. The cloud type dependent algorithms are numbered 0 to 4, where algorithm 0 represents a cloud type independent, overall algorithm. Algorithm 0 can be configured for any cloud type. More detail can be found in Thoss 2002.

For each configuration of input channels different linear combinations of those features most related to precipitation have been tested and optimized to form a precipitation index PI. For each cloud type, it was investigated which spectral features were most correlated with precipitation. A Precipitation Index PI is constructed as a linear combination of those spectral features which are most correlated with precipitation. For the day 3B and the night algorithm we have chosen a Precipitation Index of the form:

$$PI = a0 + a1 \times T_{sfc} + a2 \times T11 + a3 \times \ln\left(R0.6/R3.7\right) + a4 \times (T11 - T12) \qquad Eq\ 5$$

where a3 set to zero for the night algorithm. The coefficient values for a0-4 are given in Table 7.

Algorithm	cloud type	a0	a1	a2	a3	a4
Algorithm0-day 3B	all cloud types	35.0	0.644	-0.644	5.99	-3.93
Algorithm1-day 3B	medium level cloud	10.0	1.87	-1.87	8.43	-9.00
Algorithm2-day 3B	high opaque cloud	35.0	0.645	-6.45	9.23	-6.39
Algorithm3-day 3B	Cirrus	325.0	0.0	-1.02	5.61	-3.67
Algorithm4-day 3B	Cirrus over lower cloud	323.0	0.0	-1.00	6.00	-15.9
Algorithm0-night	all cloud types	22.0	0.863	-0.863	0.0	-6.04
Algorithm1-night	medium level cloud	0.0	2.58	-2.58	0.0	14.2
Algorithm2-night	high opaque cloud	2.0	1.10	-1.10	0.06	12.3
Algorithm3-night	Cirrus	358.0	0.0	-1.20	0.0	-2.77
Algorithm4-night	Cirrus over lower cloud	333.0	0.0	-1.00	0.0	-22.5

Table 7: Coefficients a0 to a4 for the day 3B and night algorithms.

For the construction of the PI (equation 1) the 0:8 µm channel was not considered, since its correlation with the 0.6 µm channel was very high. Introducing the NWP surface temperature - T11 in equation 1 has the advantage of reducing the seasonal dependency of the T11 term. For cirrus classes however, it was better not to consider the surface temperature and thus to set coefficient a1 to zero. The R0.6/R3.7 feature is strongly influenced by microphysical features at the cloud top, such as particle phase and size. The 3.7µm reflectivity is derived using the 11µm channel to correct for the thermal contribution. This term seems however to display a seasonal dependence, which have not yet been corrected. The T11-T12 term accounts for reduced likelihood of precipitation with reduced opacity. Coefficients a0 to a4 were calculated by maximising the correlation with precipitation class. Finally, the PI was scaled in a way that it falls into a range of approximately 0-100 for realistic input values. The current values of the coefficients of the cloud type dependent day and night algorithms are given in Table 1. When using the 1.6µm channel, it was more advantageous to use R0.6=R1.6 than the logarithm of this ratio. Since the precipitation likelihood of the R0.6=R1.6 feature does not fall monotonously, we used its distance from the approximate minimum. We also included the direct use of R0.6 as a separate feature. The Tsfc-T11 feature is only used in the algorithm for medium level clouds, and plays a minor role even there. All day time algorithms using 1.6µm are dominantly using the R0.6=R1.6 feature. Accordingly the daytime algorithms including 1.6µm showed a higher correlation with precipitation than the daytime algorithms using 3.7µm. The PI of the 3A day time algorithm is of the following form:

$$PI = a0 + a1 \times abs\left(a2 - {R0.6}/{R3.7}\right) + a3 \times R0.6 + a4(T11 - T12) + a5 \times T_{sfc} + a6 \times T11 \qquad \textit{Eq 6}$$

Coefficients a0 to a6 are given in Table 8.

While the algorithms allow a somewhat better delineation of precipitation than the night algorithm, it is anyhow recommended to use the night algorithm in case MW data is available. This is partly for guaranteeing a uniform algorithm performance day and night, partly because the day algorithms sometimes miss real precipitation. The histograms for all algorithms show that the precipitation and no precipitation classes are overlapping substantially, an example for the night algorithm is given in Figure 7.

Algorithm	A0	A1	A2	A3	A4	A5	A6
Alg. 0, all precip. ct	65.0	-15.0	4.45	0.495	-0.915	0.0	0.0
Alg. 1, medium level	60.0	-15.0	4.30	0.255	-0.800	0.17	-0.17
Alg. 2, high/very high opaque	45.0	-16.0	4.43	0.420	-0.380	0.0	0.0
Alg. 4, Ci above lower	70.0	-20.0	4.17	0.720	-0.300	0.0	0.0

Table 8: Coefficients a0 to a6 for the day 3A algorithms.

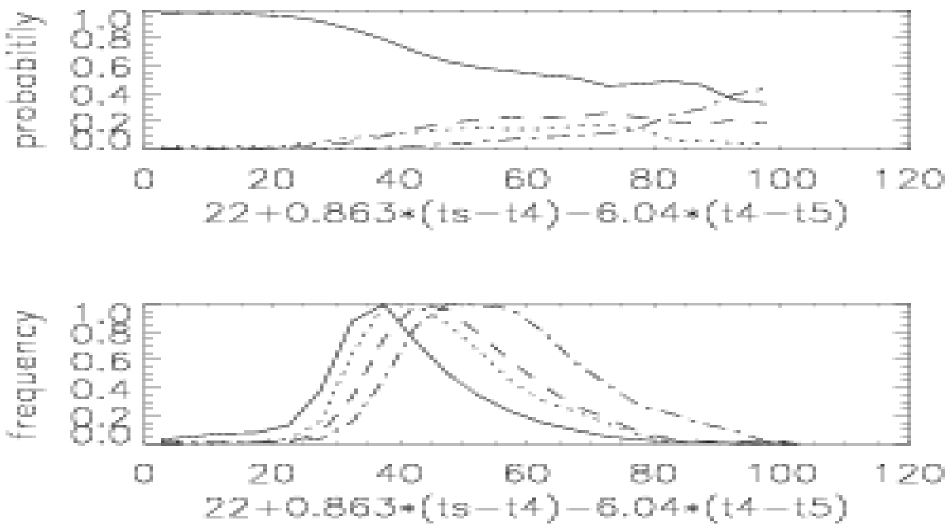

Figure 7: Precipitation index for AVHRR night algorithm for all precipitating cloud types. Upper: Probability distribution of the PI for all precipitation intensity classes. Lower: normalized frequency distribution of the PI for all precipitation intensity classes .Solid line: no rain, dotted: light, dashed: moderate, dash-dot: heavy precipitation. Delineation of intensity class requires strong convection (PI>80)

3.4 VALIDATION

An extensive validation of PGE04 was done for version 1.3, (see [RD.2]) after the software was updated in June 2007. Among other things, a new method of calculating the brightness temperature was implemented as well as new land and water SI LUT. The resulting product was smoother and more spatially accurate but the verifications scores remained poor when examined on a pixel basis and for each satellite and season. The POD was calculated on a rain/no rain, according to the Product Requirement Table for NWCSAF products, and compared to the threshold and target accuracies for the PPS/PGE04. Version 1.3 now meets and exceeds the threshold accuracy in all classes while the previous version (1.2) did not.

An examination of the two versions for each satellite included in the study as well as for different seasons showed only a slight improvement with version 1.3. The verification scores, when done more comprehensively, showed that FAR and POFD were slightly degraded, thus improvement from v1.2 to 1.3 was overall slight to moderate.

.

Probability Of Detection for all seasons, satellites, and entire year

	Product Requirement Table			
Precipitation Class	Threshold Accuracy	Target Accuracy (SeSp)	PGE04 v1.2	PGE04 v1.3

No PCPN	70%	80%	89%	83%
Light PCPN	50%	60%	44%	55%
Moderate + Heavy PCPN	60%	70%	61%	68%

Table 9: Probability Of Detection for all season, satellites, and entire year. This is compared to the Product Requirement Table for SAFNWC products.

PGE04 Version 1.3 NOAA18 for NWCSAF/PPS v2008					
Probability Classes Threshold 10					**No. Obs**
No PCPN	78.86%	11.68%	9.16%	0.29%	243900596361
Light	35.41%	26.47%	35.39%	2.73%	16228086481
Moderate	26.04%	20.89%	45.75%	7.32%	13387865139
Heavy	23.71%	11.8%	49.62%	14.87%	1085297322
Probability Classes Threshold 20					
No PCPN	82.84%	9.6%	7.27%	0.29%	243900596361
Light	43.79%	22.15%	31.32%	2.73%	16228086481
Moderate	32.37%	17.65%	42.65%	7.32%	13387865139
Heavy	27.97%	9.64%	47.52%	14.87%	1085297322
Probability Classes Threshold 30					
No PCPN	85.82%	8.37%	5.51%	0.29%	243900596361
Light	51.7%	19.89%	25.68%	2.73%	16228086481
Moderate	39.4%	16.24%	37.03%	7.32%	13387865139
Heavy	32.96%	9.23%	42.94%	14.87%	1085297322
Probability Classes Threshold 40					
No PCPN	89.71%	6.93%	3.07%	0.29%	243900596361
Light	65.06%	17.15%	15.06%	2.73%	16228086481
Moderate	54.33%	14.55%	23.79%	7.32%	13387865139
Heavy	46.06%	8.69%	30.38%	14.87%	1085297322

Probability Classes Threshold 50					
No PCPN	93.44%	4.26%	2.01%	0.29%	243900596361
Light	75.11%	11.98%	10.18%	2.73%	16228086481
Moderate	67.18%	10.95%	14.59%	7.28%	13387865139
Heavy	63.79%	7.05%	14.58%	14.59%	1085297322
Probability Classes Threshold 60					
No PCPN	95.36%	2.37%	1.98%	0.29%	243900596361
Light	79.75%	7.44%	10.08%	2.73%	16228086481
Moderate	71.24%	7.23%	14.25%	7.28%	13387865139
Heavy	67.62%	4.86%	12.96%	14.56%	1085297322

Table 10: Contingency table for the NOAA18 satellite for one year and a threshold of 10-60% using PPS version 2008. It demonstrates the algorithm performance under the simplifying assumption that all data exceeding the threshold for total precipitation likelihood is precipitating. The data is then assigned to the precipitation class with the largest likelihood The table is colour coded such that red = misses, blue = false alarms, grey = hits, and green = correct negatives.

4. KNOWN PROBLEM AREAS AND LIMITATIONS

Changes along the scanline of surface emissivity for land or water surfaces are not accounted for. If, for example, to the left side of the scan sea ice is present, and to the right side open water, the algorithm will assign a mixture of both to determine the background. This will lead to misclassifications. There seems be scope to further improve background brightness temperature estimation taking into account more than one scanline at a time or by using averages over several overpaths (Antonelli, 2007), and thus contribute to a better separability of classes. Snow cover is known to give high scattering signatures similar to precipitation in some cases, depending on the change in emission properties of the snow surface. These properties have been known to be varying even from one overpass to the next. Since this scattering is in many cases not present at all, it was decided not to generally screen out snow.

Note, that changes in land surface temperature are *not* as important as changes in surface emissivity, since the precipitation classification algorithm uses temperature differences between 89 GHz and 150 GHz and not absolute temperatures.

The MW part of the algorithm is dependent on scattering at large ice particles. For this reason there are limitations to extend this algorithm to regions where precipitation is building up without undergoing an ice phase.

Tuning of the product has been done with NORDRAD/Baltrad radar data. The algorithm seems to perform similarly over other parts of Europe, but more quantitative validation is needed here.

For GAC and Global Metop datasets there are no data available corresponding to AMSU data, therefore only a PC product with limited quality can be processed. For data from the NPP satellite there has not yet been any development done to use any data corresponding to AMSU data, thus also there only a PC product with limited quality can be processed.

5. PRACTICAL CONCIDERATIONS

5.1 PC INPUTS

Satellite data

The PC product makes use of all AVHRR channels except for the 0.8 µm channel. When use of the night time algorithm is configured, only T11 and T12 of the AVHRR will be used. AMSU use can be configured (strongly recommended). If activated, the AMSU pre-processing module will be executed once for the overpass and will calculate scattering indices derived from AMSU-B (89GHz and 150GHZ channels used). Input to the pre-processing has to be supplied as AMSU level 1c output files of the AAPP processing package. The resulting AMSU output file containing scattering indices and processing flags for the overpass is an input to the main PC module.

The PC product can take data from the NPP satellite (as well as in the future: JPPS satellites), it then uses the VIIRS channels that are corresponding to the AVHRR channels. Though the PPS is not yet prepared for taking in micro-wave data from the NPP (or JPSS) satellite, as the micro-wave data from NPP is not so corresponding to the AMSU data. Thus, running the PC product on data from NPP is like running it on AVHRR data, but without AMSU data.

Sun and satellite angles

Sun and satellite angle files are mandatory input to the PC product. Currently only the sun zenith angle is actively used by the algorithm.

Land sea mask

Land cover information is only used for the AMSU pre-processing. For this purpose a land sea mask giving the percentage of land cover in 5km resolution has been derived from USGS data.

NWP data

From NWP data only the Surface temperature field is required.

PGE02

The cloud type product, PGE02 is a mandatory input to the PC module.

5.2 CONFIGURABLE PARAMETERS

A comprehensive list of inputs, algorithm specific coefficient files etc. is given in the software user manual [RD.5]. All of those files are mandatory and should not be changed by the user. **The only file were local adjustments may be required is the model configuration file**. We will highlight here those parameters in the model configuration file that are useful to adjust to local requirements:

- Specify whether to use AMSU data or not (parameter USE_AMSU in GLOBAL_PARAM)
- Specify which processing flags you want to generate(in GLOBAL_PARAM)
- IMPORTANT: You can chose to always run the night algorithm by setting parameter SUNZEN_ANGLE in GLOBAL_PARAM to 0! This is the recommended configuration if MW data is available. Otherwise it is recommended to set that parameter to 80, which means that at a sun zenith angle lower than 80 degrees the day algorithm will be activated.
- You can choose to always run the cloud type independent algorithm 0 by modifying block CLOUDTYPE_DEFINITIONS:CLOUDTYPE the first column gives the cloud type (do not modify), in the second column is set which cloud types are checked for precipitation (0 = no precipitation, 1 = potential precipitation). If you have doubts about the algorithm performance to catch for example locally typical drizzle from low clouds, you might experiment carefully with these settings. Another candidate could be to deactivate precipitation from cirrus in summer or in case the cloud type classification for cirrus seems reliable in your area (the assumption here is that we might have misclassified fairly opaque cloud or cirrus overlaying opaque cloud as cirrus). The third column gives the algorithm ID to use. This number you can set to zero to run the cloud type independent algorithm, but make sure you can restore the original algorithm configuration! Please contact the developers via NWCSAF helpdesk in case you need more information or advice.

The other parameters are not useful for the user to modify and reserved as configurable purely for keeping flexibility for development.

5.3 OUTPUT

The output is given as precipitation likelihood for the three precipitating classes, out of the four classes. Summing up the three classes (‘light precipitation’, ‘moderate precipitation’ and ‘intense precipitation’) will give the total precipitation likelihood. The total precipitation likelihood is the most useful parameter to display in case you are not using AMSU data. With the use of AMSU data there is some skill in classifying the precipitation intensity. The likelihood output of the AVHRR algorithm is given in 10% classes. This means actually that 0% represents the interval 0 - 5%, 10% spans from 5 to 15% precipitation likelihood etc., up to 100% representing 95 - 100% likelihood.

A a post-processing step can be run, generating a file summarizing statistics for the scene. It is written in ASCII or xml and is self explanatory.

In accordance with the other PGE’s there is a common set of condition and quality flags to characterize the classification status on a pixel basis. See details below.

Condition flags

Bit Number	Description
0	Pixel is out of swath or points to space
1 and 2	Defines the illumination condition: 0: N/A 1: Night 2: Day 3: Twilight
3	Sunglint
4 and 5	Defines whether it is land or sea: 0: N/A 1: Land 2: Sea 3: Coast
6	High terrain
7	Rough terrain
8 and 9	Satellite input data status: 0: N/A 1: All satellite data are available 2: At least one useful channel is missing 3: At least one mandatory channel is missing
10 and 11	NWP input data status: 0: N/A (not classified pixel or NWP data not used) 1: All NWP data are available 2: At least one useful NWP field is missing 3: At least one mandatory NWP field is missing
12 and 13	Product input data status: 0: N/A (not classified pixel or input product data not used) 1: All product input data are available

Bit Number	Description
	2: At least one useful input product is missing 3: At least one mandatory input product is missing
14 and 15	Auxiliary data status: 0: N/A (not classified pixel or auxiliary data not used) 1: All auxiliary data are available 2: At least one useful auxiliary field is missing 3: At least one mandatory auxiliary is missing

Quality flags

Bit Number	Description
0	Pixel is NODATA
1	This bit is not used in PPS. It is a left over to keep the same bit numbers as GEO.
2	This bit is not used in PPS. It is a left over to keep the same bit numbers as GEO.
3 to 5	Retrieval quality: 0: N/A (no data) 1: Good 2: Questionable 3: Bad 4: Interpolated/Reclassified

There is also a third flag, specific for pge04. If according bit is set to 1.

Bit Number	Description
0	NWP data suspected low quality

Bit Number	Description
1	There is no reliable method for precipitating rate. (For v2014: precipitating rate is not implemented, so this bit is always set.)
2	For precipitation likelihood: AVHRR data is used
3	For precipitation likelihood: AMSU data is used
4	For precipitation likelihood: Solar channel data is used

5.4 VISUALISATION

The PC product is like the other PPS cloud and precipitation products first of all a digital product available in HDF5 which should be used together with the appended flags, e.g. as input to an automated mesoscale analysis or nowcasting scheme. When AMSU data has been used, we recommend to display the precipitation likelihood as a RGB colour composite of the intensity classes as done in Figure 8. If displaying a product from AVHRR only, we recommend however to sum up the precipitation likelihood of class one to three to the total precipitation likelihood, and then display the total precipitation likelihood using a colour coding.

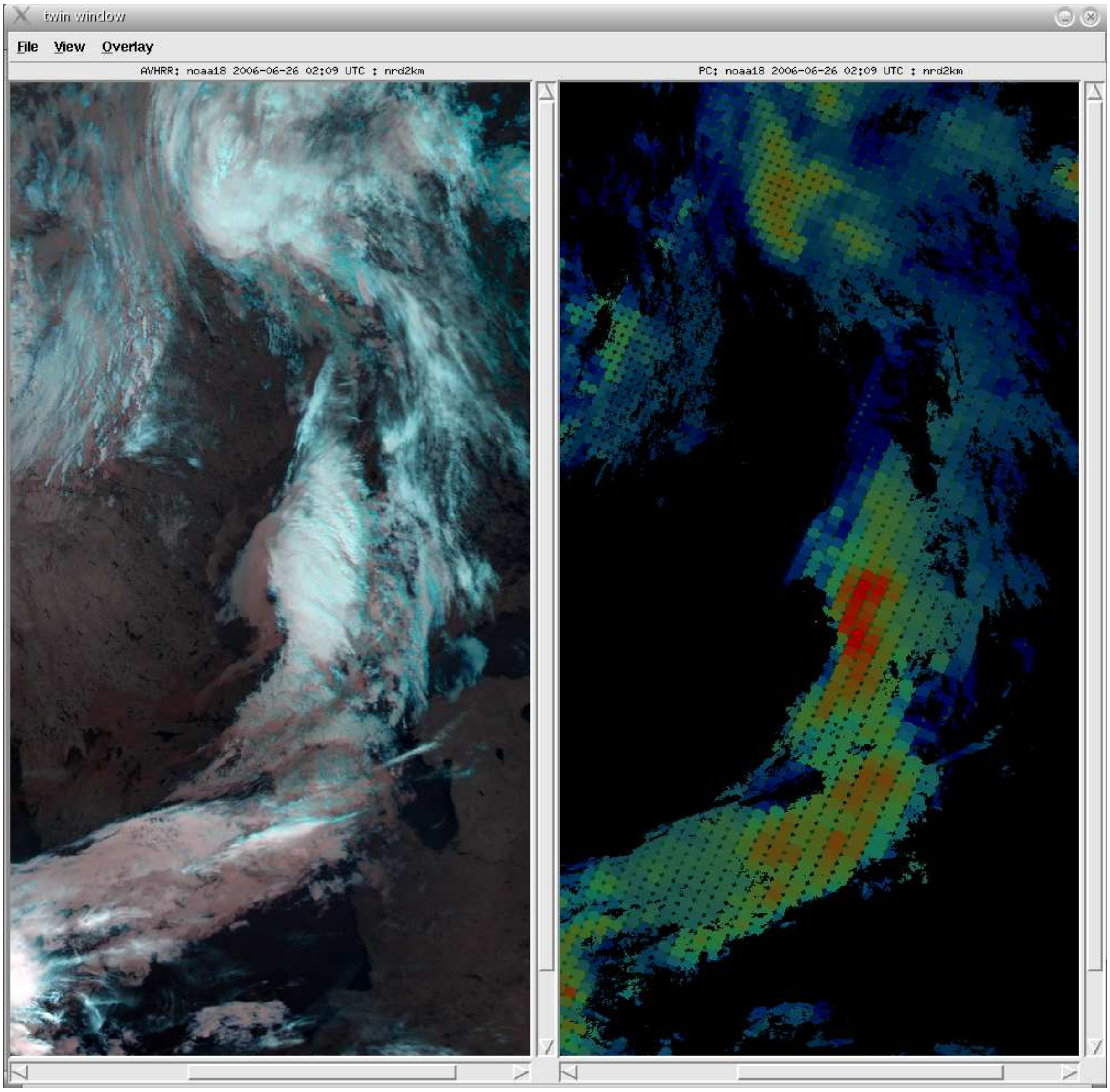

Figure 8: An example of the precipitation cloud product (left) derived from the AVHRR (RGB) (right). This scene is a NOAA18 shot taken 2006-06-26 at 0209Z. The PC product was generated using PPS version 2.1 and PGE04 version 1.3.

Example of precipitating clouds image display using a dedicated PPS image viewer developed at SMHI. To the left a close up RGB image and to the right the corresponding precipitating clouds product based on AVHRR and AMSU. Heavy precipitation is displayed as red, light to moderate precipitation as green and very light (or risk of) precipitation as blue.

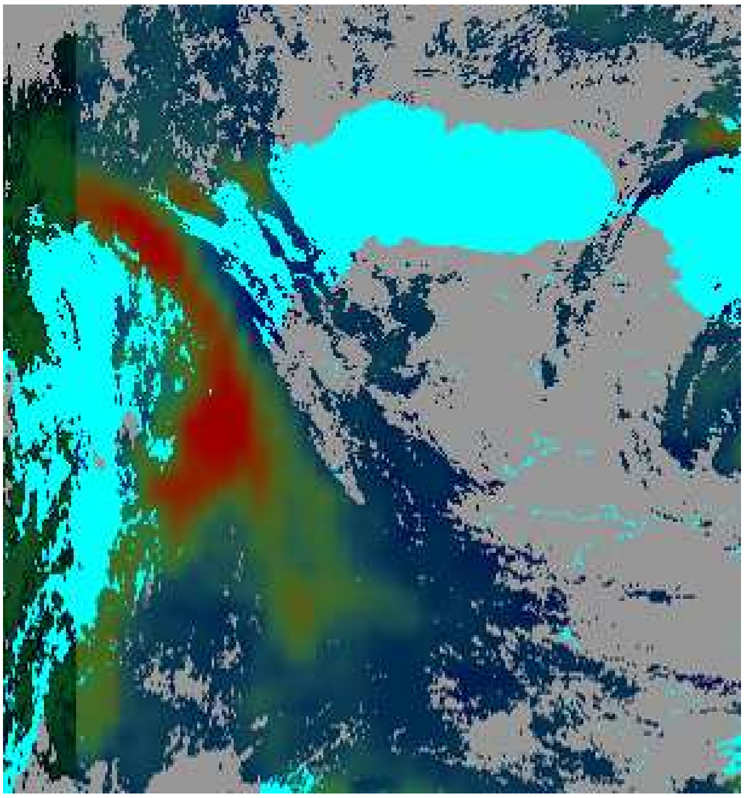

Figure 9 Example of PC product output where the switch between AVHRR algorithm and AMSU algorithm can be seen (outer part of the swath, on the left side of the image, is not covered by AMSU). The scene is NOAA19 taken 20111122 at 1336Z (over northern Africa/Spain, upside down)

For the PC product the AMSU coverage does not cover the entire region. This is dues to the different area coverage of the AVHRR and the AMSU algorithm. On both edges of a swath is missing the AMSU data, only AVHRR data is used. The remainder of the image is mostly AMSU, except for AVHRR estimates covering up in between the AMSU FOV's. In Figure 9 we see the left part of a swath, and can see the image changing character along a line close to its left side.

5.5 LIKELIHOOD THRESHOLD FOR RAIN

Since the SI for the different precipitation classes overlap so much, a threshold was set to help to delineate between dry conditions and precipitation. End-users might view the PC product as pure probabilities and as such would need a threshold for what is precipitation. The threshold is the sum of the three precipitation classes: light, moderate, and heavy. This is an attempt to quantify such a threshold that would not degrade the product quality too much.

When applied, the no-precipitation hits will increase by increasing the threshold value. But the precipitation hits category are also affected negatively. It was found that a value of 20% is sufficient to boost the cases of dry conditions without severely affecting the other categories.

ANNEX A. List of TBC, TBD, Open Points and Comments

TBD/TBC	Section	Resp.	Comment